

Super-high brightness and excellent colour quality laser-driven white light source enables miniaturized endoscopy

Shuxing Li,^a Linhui Huang,^a Yunqin Guo,^a Le Wang,^{*b} and Rong-Jun Xie^{*ac}

^aFujian Provincial Key Laboratory of Surface and Interface Engineering for High Performance Materials, College of Materials, Xiamen University, Xiamen 361005, China

^bCollege of Optical and Electronic Technology, China Jiliang University, Hangzhou 310018, China

E-mail: calla@cjlu.edu.cn.

^cState Key Laboratory of Physical Chemistry of Solid Surfaces, Xiamen University, Xiamen 361005, China

E-mail: rjxie@xmu.edu.cn

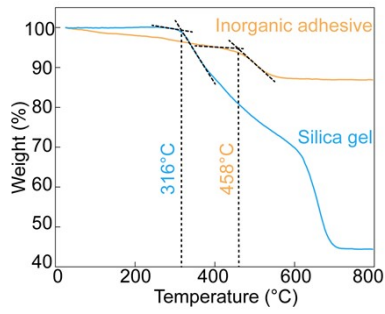


Fig. S1 Thermogravimetric analyses (TGA) of silica gel and inorganic adhesive.

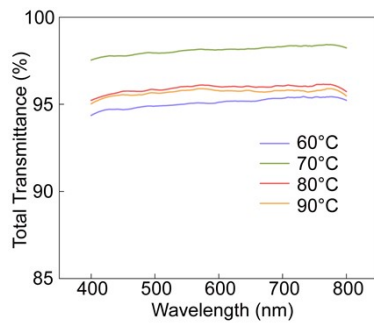


Fig. S2 Total transmittance of inorganic adhesive in the visible-light-spectrum range.

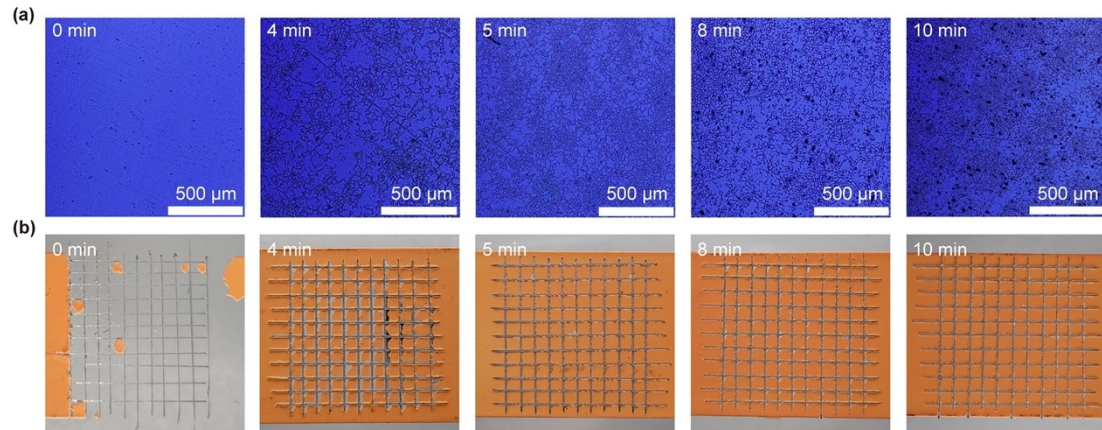


Fig. S3 (a) Surface microscope images of Al substrate by etching with alkaline for 0 ~ 10 mins, respectively. (b) Scratch test results of CASN@Al phosphor converters, where Al substrates were etched for 0, 4, 5, 8 and 10 mins, respectively.

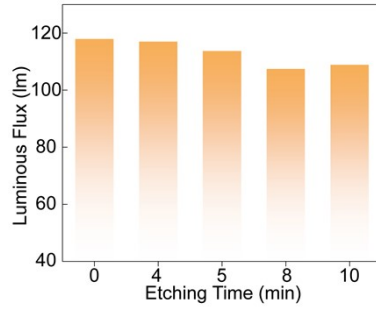


Fig. S4 Output luminous fluxes of CASN@Al phosphor converters, where Al substrates were etched for 0, 4, 5, 8 and 10 mins, respectively.

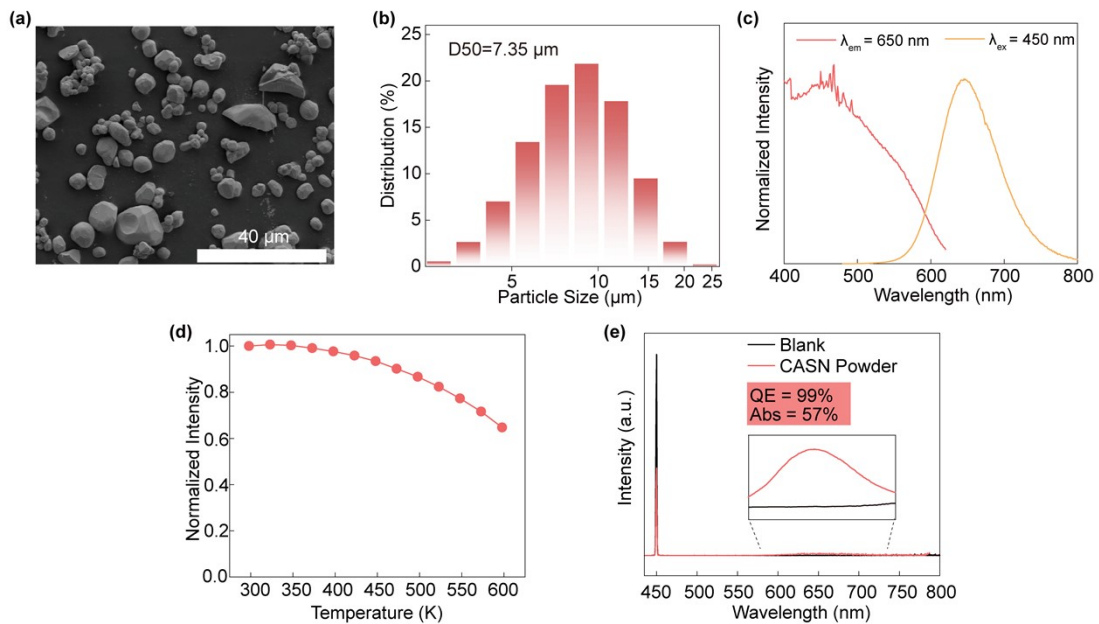


Fig. S5 Fundamental properties of CASN powders. (a) Morphology. (b) Size distributions. (c) Photoluminescence (PL) spectra. (d) Thermal quenching. (e) Quantum efficiency (QE) and absorption efficiency (Abs).

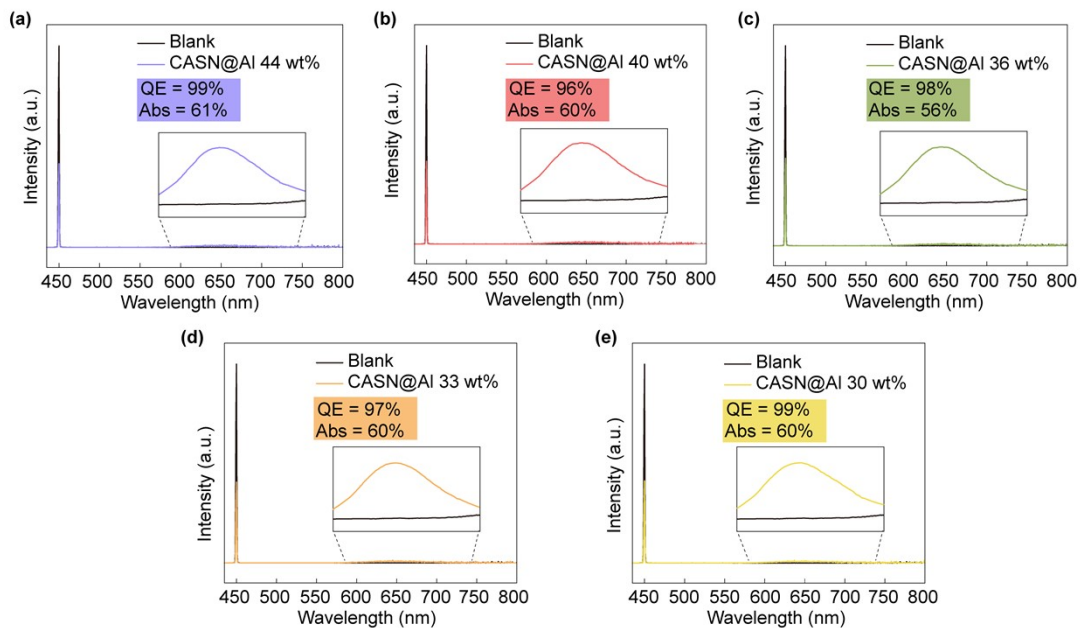


Fig. S6 Photoluminescence spectra of CASN@Al with different CSAN concentrations for QE determination.

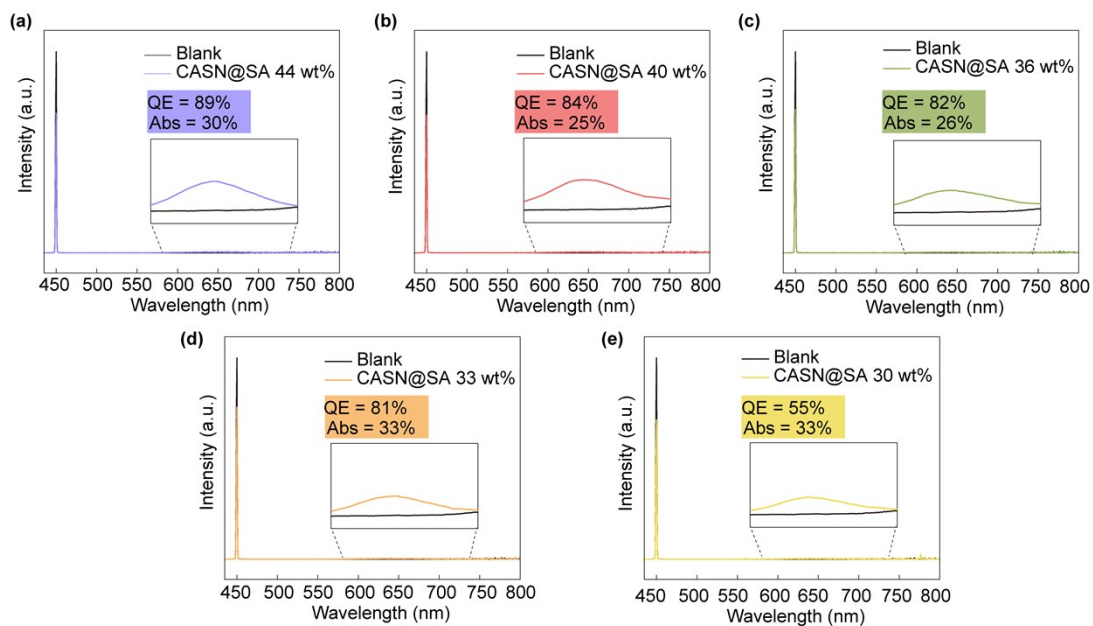


Fig. S7 Photoluminescence spectra of CASN@SA with different CASN concentrations for QE determination.

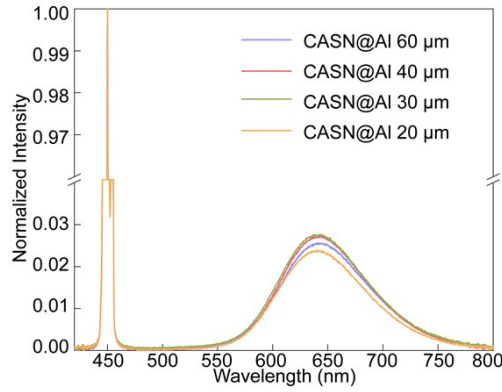


Fig. S8 Emission spectra of CASN@Al with different phosphor film thicknesses under the excitation of a laser power density of 1.22 W/mm².

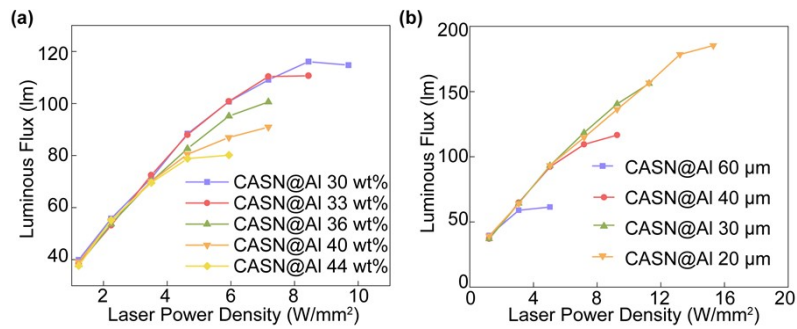


Fig. S9 Output luminous fluxes of CASN@Al with (a) different CASN concentration or (b) different film thickness as a function of incident laser power density.

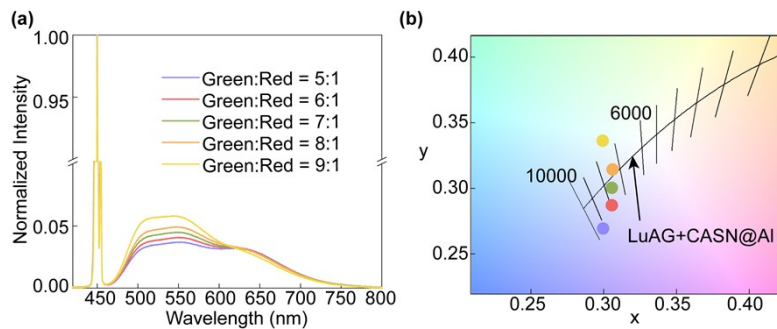


Fig. S10 Emission spectra (a) and CIE colour coordinates (b) of LuAG+CASN@Al with green to red ratios changing from 5:1 to 9:1 under the excitation of a blue laser power density of 1.22 W/mm².

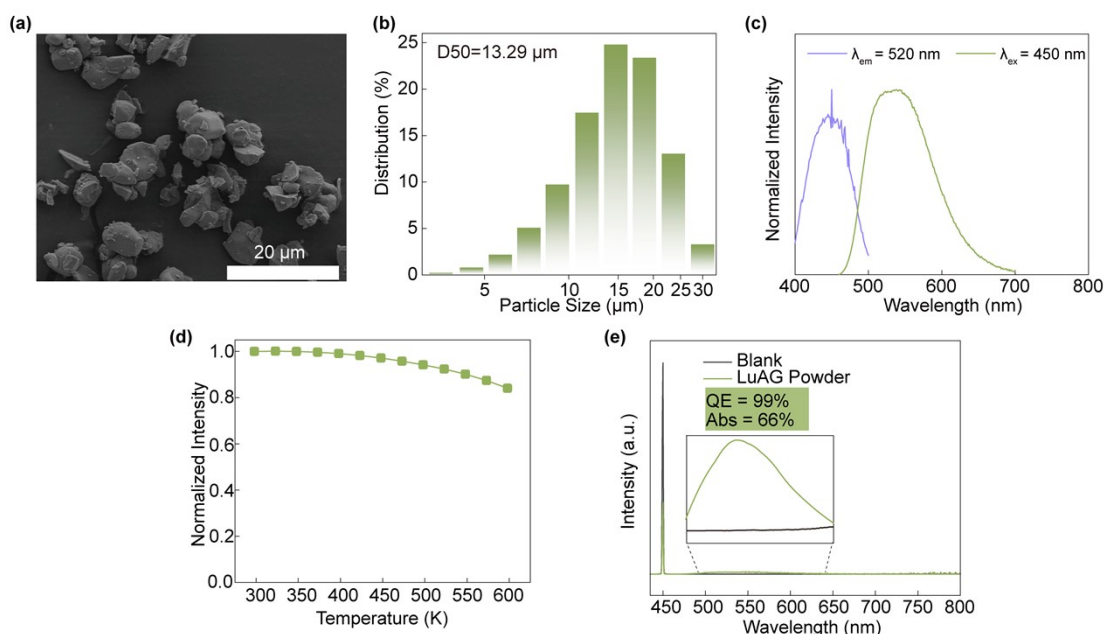


Fig. S11 Fundamental properties of LuAG powders. (a) Morphology. (b) Size distributions. (c) Photoluminescence (PL) spectra. (d) Thermal quenching. (e) Quantum efficiency (QE) and absorption efficiency (Abs).

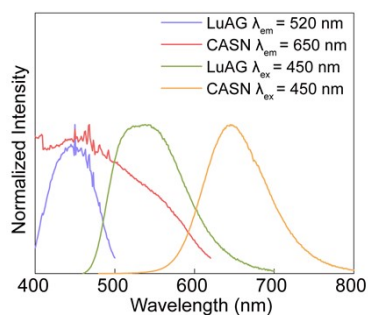


Fig. S12 Photoluminescence (PL) spectra of CASN and LuAG powders.

Table S1 QEs and absorptions of CASN@Al and CASN@SA with different phosphor concentrations.

CASN concentration (wt%)	CASN@Al		CASN@SA	
	QE (%)	Absorption (%)	QE (%)	Absorption (%)
30	99	67	89	33
33	96	67	84	33
36	98	74	82	26
40	97	75	81	25
44	99	70	55	30

Table S2 Luminous flux and luminous efficacy of LuAG+CASN@Al and LuAG/CASN@Al under excitation of incident blue laser power density increasing from 1.22 to 5.94 W/mm².

Laser power density (W/mm ²)	LuAG+CASN@Al		LuAG/CASN@Al	
	Luminous flux (lm)	Luminous efficacy (lm/W)	Luminous flux (lm)	Luminous efficacy (lm/W)
1.22	133	217	158	258
2.24	194	173	220	196
3.50	259	148	294	168
4.64	326	140	365	157
5.95	384	129	433	146

Table S3 A summary of luminous flux and luminous efficacy of reported laser-driven white light sources with Ra above 90.

	Luminous flux (lm)	Luminous efficacy (lm/W)	Refs	Notes*
1	288	102	[17]	Transmissive surface
2	404	137	[19]	Total surfaces
3	183	85	[20]	Total surfaces
4	110	120	[21]	Transmissive surface
5	220	121	[22]	Total surfaces
6	373	106	[23]	Transmissive surface
7	433	146	This work	Reflective surface

*According to the optical configuration, white light is collected on either the transmissive or reflective surface of the phosphor relative to the incident direction of blue laser. It is worth mentioning that the total luminous flux, collected from all surfaces of the phosphor, is unsuitable as a reference for practical applications of laser-driven white light sources.